Energetic Electrons in the Midlatitude Nighttime E Region

L. G. Smith, M. A. Geller, and H. D. Voss

Aeronomy Laboratory, Department of Electrical Engineering,

University of Illinois, Urbana, Illinois 61801

Abstract-Nike Apache 14.439 was launched from Wallops Island at 0003 EST on 1 November 1972, a very disturbed night (K_p = 8). A Geiger counter in the payload detected electrons (>70 keV) with a maximum flux of 1086 ± 26 $cm^{-2}sec^{-1}ster^{-1}$. The height-averaged ionization rate in the upper E region is calculated from the measured electron density profile and has a value of 35 $cm^{-3}sec^{-1}$. This ionization rate can be reconciled with the observed flux of electrons (>70 keV) if the spectrum (>2 keV) is of the form $J(>E) = J_o \exp(-E/E_o)$ with E_o equal to 8.3 keV. The ionization rate on this and other nights is found to be strongly dependent on geomagnetic activity. It is suggested that energetic electrons are the principal source of ionization at midlatitudes in the upper E region near midnight, even under rather quiet geomagnetic conditions.

1. Introduction

Rocket observations at Wallops Island (38°N, 75°W; geomagnetic latitude 49°N) have shown the presence of a layer in the upper E region near midnight (Cartwright, 1964; Smith, 1970). This intermediate layer is formed by the vertical redistribution of ionization under the influence of the neutral winds

(Constantinides and Bedinger, 1971; Fujitaka et. al., 1971; Chen and Harris, 1971). The source of ionization has been presumed to be solar UV radiation resonately scattered by the geocorona, principally Lyman-α (1216 A), which ionizes nitric oxide (Swider, 1965) and Lyman-β (1026 A), which ionizes molecular oxygen (Ogawa and Tohmatsu, 1966).

The possibility exists, particularly on disturbed nights in the sub-auroral zone (geomagnetic latitude 45° to 60°), that energetic electrons provide an additional source of ionization in the upper E region and can therefore influence the intermediate layer (Manson, 1971). The rocket experiment which is described here was undertaken to examine the role of energetic electrons as a source of ionization in the midlatitude nighttime ionosphere. The rocket launch time was chosen to be midnight to minimize the effect of UV sources of ionization and the launch held for a night of considerable geomagnetic activity.

After presenting the observations from this rocket launch, we consider the interpretation of the observed enhancement in electron density and deduce a flux of electrons with energies in the range 2 to 10 keV necessary to explain the effect. This flux is shown to be reasonable for the disturbed conditions of that night.

In a later section of the paper we consider previous observations of the intermediate layer near midnight. Making proper allowance for the vertical redistribution of ionization resulting from the effect of the horizontal neutral wind, we deduce the average ionization rate of the upper E region. This is found to be well correllated with the planetary index of geomagnetic activity, which leads us to suggest that, near local midnight, energetic electrons are an important source of ionization in the upper E region, not only on disturbed nights but also for quiet conditions.

2. Instrumentation

Nike Apache 14.439, instrumented to obtain the electron density profile and to measure the flux of energetic electrons, was launched from Wallops Island, Virginia, at 0003 EST (0503 UT) on 1 November 1972, during a magnetic storm. The value of K_p for the three-hour interval (03-06 UT) including the launch time was 8. The rocket achieved an apogee of 195.6 km and, in mid-flight had a spin rate of 7.3 rps.

The payload included a Langmuir probe using the nose tip electrode (Smith, 1969). This is operated at a fixed potential of +4.05 volt until 100 sec after launch (127 km altitude). For the remainder of the flight the probe alternates between the fixed-voltage mode of 1.5 sec duration and a swept mode of 0.5 sec duration. The constant of proportionality between probe current in the fixed-voltage mode and electron density changes with altitude and varies from flight to flight. The probe is therefore calibrated in flight by a propagation experiment. For this flight two frequencies were used: 2225 kHz and 3385 kHz. The propagation experiment at each frequency uses differential absorption and Faraday rotation data (Mechtly and Smith, 1970).

The payload also included a Geiger counter with a window of beryllium, area 0.203 cm^2 and thickness 5.1×10^{-3} cm. The counter was originally designed for measurement of the daytime flux of solar X-rays in the wavelength range 1 to 8 A (Accardo et. al., 1972). It is also sensitive to electrons with energies greater than 70 keV, for which the geometric factor is 0.303 cm^2ster. Although such relatively high-energy electrons are important only in the D region the counter was included in the payload as a direct indicator of a particle precipitation event. The window of the Geiger counter is oriented perpendicular to the spin axis of the rocket and is covered, during the launch phase, by a door carrying a weak radioactive source. The door and source are ejected 41 sec after launch (43 km altitude).

3. Observations

3.1 Flux of energetic electrons

The count rate measured during the flight is shown in Figure 1. Each data point is the average for a five-second interval. The uncertainty in count rate is indicated by error bars at representative points. The data below 60 km on the descending trajectory are of poor quality and are not included in the figure.

The count rate of the detector at sea-level (before launch) is 3.3 sec^{-1}, of which the source on the door contributes 3.0 sec^{-1} and the cosmic-ray background 0.3 sec^{-1}. The dashed line in Figure 1 connects points which have been corrected for the radioactive source carried in the early part of the flight. The resulting variation with altitude up to about 80 km, including the Pfotzer-Regener maximum near 20 km, is consistant with previous observations of cosmic ray fluxes at midlatitudes (Van Allen and Tatel, 1948). In other (daytime) flights with identical counters the background count rate, due to cosmic rays, has been found to be about 10 sec^{-1} at altitudes greater than 40 km.

The excess counts on this flight are attributed to electrons with energies greater than 70 keV. The flux increases with increasing altitude in the range 80 to 140 km both on ascent and descent. While the rocket is above 140 km there is no obvious relation with altitude, the flux being variable and gradually decreasing. The count rate reaches a maximum value of 339 ± 8 sec^{-1}, which, when corrected for cosmic rays, gives a flux (>70 keV), assumed isotropic, of 1086 ± 26 cm^{-2} sec^{-1} $ster^{-1}$. In the period that the rocket is above 140 km the minimum flux is 132 ± 9 cm^{-2} sec^{-1} $ster^{-1}$. These fluxes have been compared

with other midlatitude data collected by Potemra and Zmuda (1970) and are found to be close to their upper limit, confirming that this occasion was very disturbed.

3.2 Electron Density

The electron density profile from this flight is shown in Figure 2, together with that from Nike Apache 14.394, also launched at Wallops Island near midnight, but on a much quieter night (K_p: 2+). The earlier profile is typical of previous observations of the E region near midnight. The main features of these are the lower irregular region between 90 and 110 km, the valleys at about 120 and 180 km, with the intermediate layer between. The profile from the disturbed night shows a generally greater electron density except between 93 and 105 km with much irregular structure present in the upper part of the profile. There is some indication of the intermediate layer but its presence is not as obvious as in any previous profile.

It is clear that the enhancement below 93 km is caused by energetic electrons. In the subsequent sections of this paper we shall examine the possibility that energetic electrons also are responsible for the enhancement above 105 km. That there is no substantial enhancement between these two altitudes is tentatively explained by the presence of a source of ionization from meteors, which predominates in the range 93 to 105 km. The present paper is, however, limited to detailed consideration of the region above 105 km.

4. Analysis

4.1 Introduction

Neutral winds plan an important role in determining the electron density profile of the nighttime E region. In this section, we illustrate the formation of the intermediate layer by solving the continuity equation for an assumed wind structure. Then we show that, by suitable manipulation of the

continuity equation, we may perform the inverse procedure and obtain the ionization rate, without assuming a value for the vertical ion drift velocity.

4.2 Effects of winds in the E region

The steady-state continuity equation for electrons in the E region is:

$$q - \alpha N^2 - \frac{d}{dz}(Nw) + \frac{d}{dz}\left(D\frac{dN}{dz}\right) = 0 \qquad (1)$$

in which q is the ionization rate, α is the recombination coefficient, N is the electron density, w is the vertical ion drift velocity, D is the ambipolar diffusion coefficient and z is the altitude. The small gravitational diffusion term has been neglected.

The vertical ion drift velocity is produced by the neutral wind and can be calculated using the formulation of MacLeod (1966). Electric fields may also contribute to the vertical ion drift velocity; the subsequent analysis is independent of the mechanism producing vertical ion drift, however.

For purposes of illustrating the effect of winds in the upper E region we have taken a model in which the vertical ion drift velocity, at altitudes between 120 and 180 km, is given by

$$w = 20\sin[\pi(150 - z)/30] \qquad (2)$$

where w is in m sec^{-1} and z is in km. This forces the peak to be located at an altitude of 150 km and the valleys to be located at altitudes of 120 km and 180 km. The choice of a maximum vertical velocity of 20 m sec^{-1}, is based on the work of Constantinides and Bedinger (1971).

The steady-state continuity equation (1) has been solved numerically using the Runge-Kutta technique. For simplicity both α and D have been given values appropriate to 150 km: $\alpha = 1.90 \times 10^{-7}$ $cm^3 sec^{-1}$ (Fujitaka et al., 1971) and $D = 2 \times 10^8$ $cm^2 sec^{-1}$. The latter is twice the molecular diffusion coefficient given by Golomb and MacLeod (1966).

The solution is shown in Figure 3 for five values of ionization rate: (1) 0.4, (2) 4.0, (3) 40, (4) 400 and (5) 4000 cm^{-3} sec^{-1}. The effect of omitting the diffusion term in the continuity equation is represented by the thin line. The full solution, with diffusion, is shown by the thick line. The difference is most noticable for the smaller production rates, as on quiet nights, and is completely negligible for the largest production rate, which is representative of daytime conditions. It is important to note that diffusion cannot be neglected in analysis of the intermediate layer at night.

This figure confirms that the wind becomes less effective in determining the electron density profile as the production rate increases, explaining, at least qualitatively, why the intermediate layer was less obvious on the disturbed night.

Profiles of electron density, such as those shown in Figure 3, may be analyzed to obtain the ionization rate. This has previously involved a tedious modelling procedure. The new method described here follows from integration of the continuity equation between suitably chosen limits of altitude. It does not require independent knowledge of the vertical ion drift velocity. The ionization rate is determined as the height-integrated value appropriate to the range of altitude.

4.3 Calculation of ionization rate

Consider the steady-state continuity equation (1) integrated between the altitude limits z_1 and z_2:

$$\int_{z_1}^{z_2} (q-\alpha N^2)dz - \left[Nw\right]_{z_1}^{z_2} + \left[D\frac{dN}{dz}\right]_{z_1}^{z_2} = 0 \qquad (3)$$

Reference to the calculated profiles of Figure 3 shows that the extrema of electron density (i.e. $\frac{dN}{dz} = 0$) occur at nodes of the vertical ion drift velocity (i.e. $w = 0$). Thus, if the limits of integration are altitudes z_1 and z_2, which are extrema of electron density and nodes in the vertical ion drift velocity, the terms in square brackets in equation (3) are zero at both limits. Therefore:

$$\int_{z_1}^{z_2} q\ dz = \int_{z_1}^{z_2} \alpha N^2 dz \qquad (4)$$

Thus, the height-integrated ionization rate in the layer is obtained without assuming any model for the vertical ion drift velocity. The proper choice of limits of integration has enabled us to average out the effect of vertical ion drift (whether caused by neutral winds or electric field, or both) and diffusion; they have not been neglected.

In the absence of further information or assumption about the variation of ionization rate with altitude it is convenient to define an average ionization rate given by:

$$\bar{q} = \frac{1}{(z_2 - z_1)} \int_{z_1}^{z_2} (\alpha N^2)\ dz \qquad (5)$$

The conditions for the limits of integration are met at both lower and upper valleys and at the peak of the layer. Thus the average ionization rate may be computed for (1) the layer below the peak, (2) the layer above the peak, and (3) the whole layer.

Further discussion of this method of analysis and its extension to obtain the vertical ion drift velocity are given in Geller et al. (1974).

5. Discussion

5.1 Ionization rate on the disturbed night

At night, in the altitude range of interest here, the principal ion is NO^+ (Holmes et al., 1965). The loss process is dissociative recombination of NO^+, the coefficient (α) being given by $4.5 \times 10^{-7}\ (300/T_e)\ cm^3\ sec^{-1}$ (Biondi, 1969). The electron temperature (T_e) above 120 km varies with altitude and geomagnetic activity. For purposes of calculation we have used data from Evans (1973) at Millstone Hill and find that the nighttime (2100-0300 EST) electron temperature at 200 km can be well represented by $(112\ K_p + 588)°K$ for eight occasions in 1966 and 1967 with a range of values of K_p of 1- to 5-. The correlation coefficient is 0.90. Following Evans we assume $T_e = 355°K$ at 120 km. Then a linear interpolation between these two altitudes gives

$$T_e(z) = (z - 120) \times (1.40\ K_p + 2.91) + 355°K. \qquad (6)$$

Using Biondi's formula for α and allowing the extrapolation of electron temperature to $K_p = 8$ we obtain α as a function of altitude and geomagnetic index.

This value of α has been used in integrating the electron density profile according to equation (5) to obtain the ionization rate. For the profile of 1 November 1972 between the altitudes 115 and 175 km, the ionization rate is found to be $35\ cm^{-3}\ sec^{-1}$.

5.2 Electron energy spectrum

Calculations such as those by Rees (1963) show that electrons with energies in the range of 2 to 10 keV are the most efficient as a source of ionization in the upper E region, at about 140 km. In this range of energy the ionization rate for unit flux is about 1×10^{-5} cm^{-3} sec^{-1}. Thus to produce an ionization rate of 35 cm^{-3} sec^{-1} requires a flux of electrons, with energies between 2 and 10 keV, of about 3.5×10^{6} cm^{-2} sec^{-1} $ster^{-1}$.

The energy spectrum of electrons between 2 and 70 keV was not observed on the rocket flight; there is a possibility that it may eventually be obtained from satellite data. However, in order to continue the discussion we make the assumption that the spectrum is exponential, typical of soft auroral radiation, having the form $J(>E) = J_o \exp(-E/E_o)$. Then, using the flux between 2 and 10 keV, deduced from the ionization rate, and the measured flux (>70 keV) of 1×10^{3} cm^{-2} sec^{-1} $ster^{-1}$, we find that $J_o = 4 \times 10^{6}$ cm^{-2} sec^{-1} $ster^{-1}$ and $E_o = 8.3$ keV, for E in units of keV. This value of E_o is within the limits of other observations of auroral spectra in the energy range, thus giving confidence to the assumed form of the spectrum.

The specification of the spectrum allows the flux of electrons (>40 keV) at the time of our rocket flight, with $K_p = 8$, to be estimated as 3×10^{4} cm^{-2} sec^{-1} $ster^{-1}$. This may be compared with a rocket observation by Gough and Collin (1973) at South Uist, geomagnetic latitude 58°: on one occasion, with $K_p = 8+$, they found the flux (>40 keV) to be 1×10^{4} cm^{-2} sec^{-1} $ster^{-1}$. The difference between these two values is small considering the variability of the flux. Thus the agreement is considered satisfactory.

5.3 Ionization rate on other nights

We believe, as was just discussed, that the ionization source for the upper E region on the very disturbed night can be identified as energetic electrons. It is interesting to consider next the extent to which energetic electrons contribute to the ionization on other, quieter, nights. There are now five observations of the intermediate layer at Wallops Island near midnight: 12 April 1963 (Cartwright, 1964); 22 June 1965 and 22 February 1968 (Smith, 1970); and 11 September 1969 and 1 November 1972, shown here in Figure 2.

Applying the method of analysis described in section 4.3, we have derived the ionization rate for each of these five cases, for the lower and upper parts of the layer, and for the whole layer. These values are given in Table 1, which also includes the altitudes of the valleys and the peaks used as limits in the integration of the continuity equation, and the values of K_p for the three-hour period including the launch time.

Note the relatively small difference for a given night in values of ionization rate in the lower and upper part of the region. This implies that the ionization rate is nearly constant, at midnight, over the altitude range of 120 to 180 km. There is, however, from night to night, a variation of almost three orders of magnitude.

These ionization rates are plotted in Figure 4 against the corresponding value of K_p. The larger circles represent data from the whole layer; those of the lower and upper part are represented by smaller circles. In one case all three values coincide. The ionization rate in the intermediate layer at midnight is clearly related to the level of geomagnetic activity as represented by the least-squares fit:

$$q = 0.14 \exp(0.71 K_p) \text{ cm}^{-3} \text{ sec}^{-1}. \qquad (7)$$

The correlation coefficient for the five observations is 0.96.

If the ionization is assumed to be caused by energetic electrons, equation (7) may be interpreted as descriptive of the variation with geomagnetic activity of the flux of electrons (>2 keV) at Wallops Island:

$$J(>2 \text{ keV}) \simeq 1 \times 10^4 \exp(0.71 K_p) \text{ cm}^{-2} \text{ sec}^{-1} \text{ ster}^{-1}. \quad (8)$$

A direct test of this relation may be possible from existing satellite data; it could certainly be tested in future rocket experiments. For the present, however, we can only suggest that it is reasonable, based on comparison with a series of observations by Gough and Collin (1973). They measured the flux of electrons (>40 keV) at South Uist on 13 rocket flights and found a good correlation with geomagnetic activity. Their measured flux is related to K_p at launch time by the least-squares fit:

$$J(>40 \text{ keV}) = 5.0 \exp(0.98 K_p) \text{ cm}^{-2} \text{ sec}^{-1} \text{ ster}^{-1} \quad (9)$$

With a correlation coefficient of 0.79.

Allowing for some variation of the energy spectrum from one occasion to another, the flux of electrons (>2 keV) and the flux of electrons (>40 keV) at South Uist show similar dependence on K_p. This supports our assumption that energetic electrons are the principal source of ionization in the upper E region near midnight at midlatitudes.

5.4 Latitude variation

Rowe (1973) has presented data from Arecibo, Puerto Rico, geomagnetic latitude 30°N, which show that the electron density of the upper E region at night is rather well correlated with geomagnetic activity. In this section we consider the relation between his measurements and the rocket observations at Wallops Island.

The intermediate layer, seen regularly at Wallops Island, is not a feature of the nighttime ionosphere at Arecibo, presumably because of the

difference in wind systems at the two latitudes. The electron density at Arecibo is nearly constant in the region 130 to 160 km. We have calculated the ionization rate there from electron density data using a value of recombination coefficient which is a function of altitude and K_p, as described in section 5.1. We shall consider first a simultaneous observation of electron density at Wallops Island and Arecibo.

At our suggestion observations were made at Arecibo on the very disturbed night, 31 October - 1 November 1972. At the time of the rocket observation at Wallops Island, the electron density between 140 and 160 km at Arecibo was constant with a value of 6×10^3 cm^{-2} (Rowe, personal communication). The average recombination coefficient over this range of altitude, for $K_p = 8$, is calculated to be 1.8×10^{-7} cm^3 sec^{-1} so that, for a steady-state condition, the ionization rate is 6.5 cm^{-3} sec^{-1}. This may be compared with the value 35 cm^{-3} sec^{-1} obtained from simultaneous observations at Wallops Island. The decrease of a factor of about 5 between Wallops Island and Arecibo may be attributed to the change in latitude.

The ionization rates at Arecibo for 17 nights with various values of K_p have been calculated from the average value of electron density between 130 and 160 km, given by Rowe (1973), again using a value of recombination coefficient which includes the variation of electron temperature with altitude and K_p. We find:

$$q = 2.0 \times 10^{-2} \exp(0.77K_p) \text{ cm}^{-3} \text{ sec}^{-1} \qquad (10)$$

with a correlation coefficient of 0.79.

Comparison of the variation of ionization rate with K_p at Arecibo, as given by equation (10) with the corresponding equation (7) for Wallops Island

reveals a remarkably parallel dependence on K_p. This is surprising in view of the relatively low geomagnetic latitude of Arecibo. However, it does suggest that electron precipitation may be an important source of ionization at night even on the equator-ward side of the sub-auroral zone.

Observations at low latitudes of electrons with energies of a few keV have been reported by Hill et al. (1970) and by Hayakawa et al. (1973). The former, from rocket flights at Kauai, geomagnetic latitude 22°N, on two quiet days (K_p = 1+ and 0+), find the flux of electrons with energies between 1 and 10 keV to be about 100 cm^{-2} sec^{-1} $ster^{-1}$ at an altitude of 150 km. This flux appears to be smaller, by an order of magnitude, than the flux required to produce the ionization rate deduced from the Arecibo observations, for these very quiet conditions.

6. Conclusion

Analysis of electron density profiles in the upper E region near midnight at Wallops Island has indicated that the ionization rate is very strongly correlated with geomagnetic activity. We have interpreted this as evidence that the principle source of ionization under these conditions is energetic electrons on geomagnetically quiet nights as well as on disturbed nights. Electron density data from Arecibo indicates a similar correlation between ionization rate and geomagnetic activity. Evidence of sufficient particle precipitation to account for the deduced ionization rates at Arecibo is lacking, however. The entire subject of precipitation of energetic electrons at latitudes below the sub-auroral zone is not resolved and requires further investigation.

No additional source of ionization from scattered solar UV radiation is needed to account for the ionization rates at Wallops Island. In fact, the

present data indicate that an upper limit for ionization sources other than energetic electrons is 10^{-1} cm^{-3} sec^{-1} in the upper E region near midnight.

The observations at Wallops Island also lead to the conclusion that energetic electrons are negligible as a source of ionization in the upper E region in the daytime. Even under the most disturbed conditions, energetic electrons contribute of the order of one percent of the daytime ionization rate.

Acknowledgment - The payload was built and prepared for launch by GCA Technology Division. In particular, we wish to thank G. A. Pintal for his assistance with the experiments. We also thank D. M. Cunnold for useful discussion of the method of numerical solution for the continuity equation.

The work was supported by the National Aeronautics and Space Administration under Grant NGR 14-005-181 and, in part, by the National Science Foundation under Grant NSF GA-25660.

FIGURE CAPTIONS

Figure 1. Count rate observed on a disturbed night at Wallops Island using a Geiger counter sensitive to electrons (>70 keV).

Figure 2. Electron density profiles at Wallops Island near midnight on quiet and disturbed nights.

Figure 3. The effect of winds in the E region. Calculated for a vertical ion velocity given by $w = 20 \sin[\pi(150 - z)/30]$ m sec^{-1} for altitude z in km, with the recombination coefficient 1.9×10^{-7} cm^3 sec^{-1}, for production rates of (1) 0.4, (2) 4.0, (3) 40, (4) 400 and (5) 4000 cm^{-3} sec^{-1}. The thin line is the solution neglecting diffusion; the thick line is the complete solution with a diffusion coefficient of 2×10^8 cm^2 sec^{-1}.

Figure 4. The variation with K_p of the ionization rate in the upper E region from observations of the intermediate layer near midnight.

Table 1: Ionization Rate in the Upper E Region near Midnight.

Date	Altitude (km)			Ionization Rate (cm^{-3} sec^{-1})			
	Valley	Peak	Valley	Lower	Upper	Whole	K_p
12 Apr. 1963	120	140.5	182	0.90	0.48	0.62	1
22 Jun. 1965	125	153	177	0.090	0.071	0.081	0+
22 Feb. 1968	116	140	154	2.0	3.3	2.5	3+
11 Sep. 1969	118	148.5	180	0.60	0.59	0.59	2+
1 Nov. 1972	115	143	175	26	43	35	8

References

Accardo C. A., Smith L. G., and Pintal G. A.	1972	J. atmos. terr. Phys. 34, 613.
Biondi M. A.	1969	Can. J. Chem. 47, 1711.
Cartwright D. G.	1964	J. geophys. Res. 69, 4031.
Chen W. M. and Harris R. D.	1971	J. atmos. terr. Phys. 33, 1193.
Constantinides E. and Bedinger J. F.	1971	J. atmos. terr. Phys. 33, 461.
Evans J. V.	1973	Planet. Space Sci. 21, 763.
Fujitaka K., Ogawa T., and Tohmatsu T.	1971	J. atmos. terr. Phys. 33, 687.
Geller M. A., Smith L. G., and Voss H. D.	1973	Trans. AGU 54, 1151 (abstract).
Golomb D. and MacLeod M. A.	1966	J. geophys. Res. 71, 2299.
Gough M. P. and Collin H. L.	1973	J. atmos. terr. Phys. 35, 835.
Hayakawa S., Kato T., Kohno T., Murakami T., Nagase F., Nishimura K., and Tanaka Y.	1973	J. geophys. Res. 78, 2341.
Hill R. W., Grader R. J., Seward F. D., and Stoering P. J.	1970	J. geophys. Res. 75, 7267.
Holmes J. C., Johnson C. Y., and Young J. M.	1965	Space Res. V (Edited by D. G. King-Hele, P. Muller and G. Righini), p. 756. North-Holland, Amsterdam.
MacLeod M. A.	1966	J. Atmos. Sci. 23, 96.
Manson A. H.	1971	Planet. Space Sci. 19, 270.

Mechtly E. A. and Smith L. G.	1970	Radio Sci. 5, 1407.
Ogawa T. and Tohmatsu T.	1966	Rep. Iono. Space Res. (Japan) 20, 395.
Potemra T. A. and Zmuda A. J.	1970	J. geophys. Res. 75, 7161.
Rees M. H.	1963	Planet. Space Sci. 11, 1209.
Rowe J. F., Jr.	1973	J. geophys. Res. 78, 6811.
Smith L. G.	1969	Small Rocket Instrumentation Techniques (Edited by K. I. Maeda) p. 1. North-Holland, Amsterdam.
Smith L. G.	1970	J. atmos. terr. Phys. 32, 1247.
Swider W.	1965	J. geophys. Res. 70, 4859.
Van Allen J. A. and Tatel H. E.	1948	Phys. Rev. 73, 245.

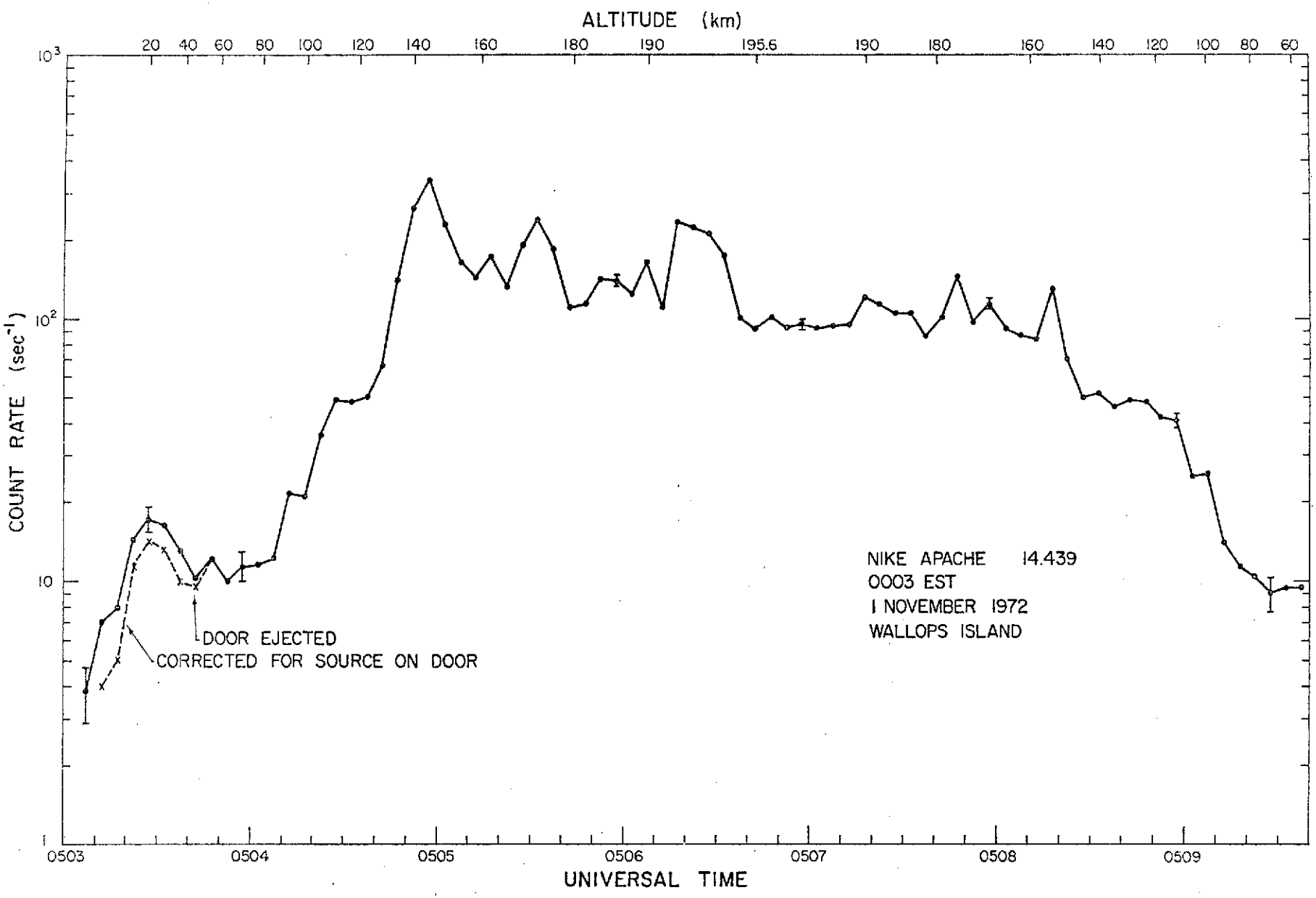
ALTITUDE (km)
20 40 60 80 100 120 140 160 180 190 195.6 190 180 160 140 120 100 80 60
10^3
10^2
10
1
COUNT RATE (sec^{-1})
DOOR EJECTED
CORRECTED FOR SOURCE ON DOOR
NIKE APACHE 14.439
0003 EST
1 NOVEMBER 1972
WALLOPS ISLAND
0503
0504
0505
0506
0507
0508
0509
UNIVERSAL TIME

Figure 1

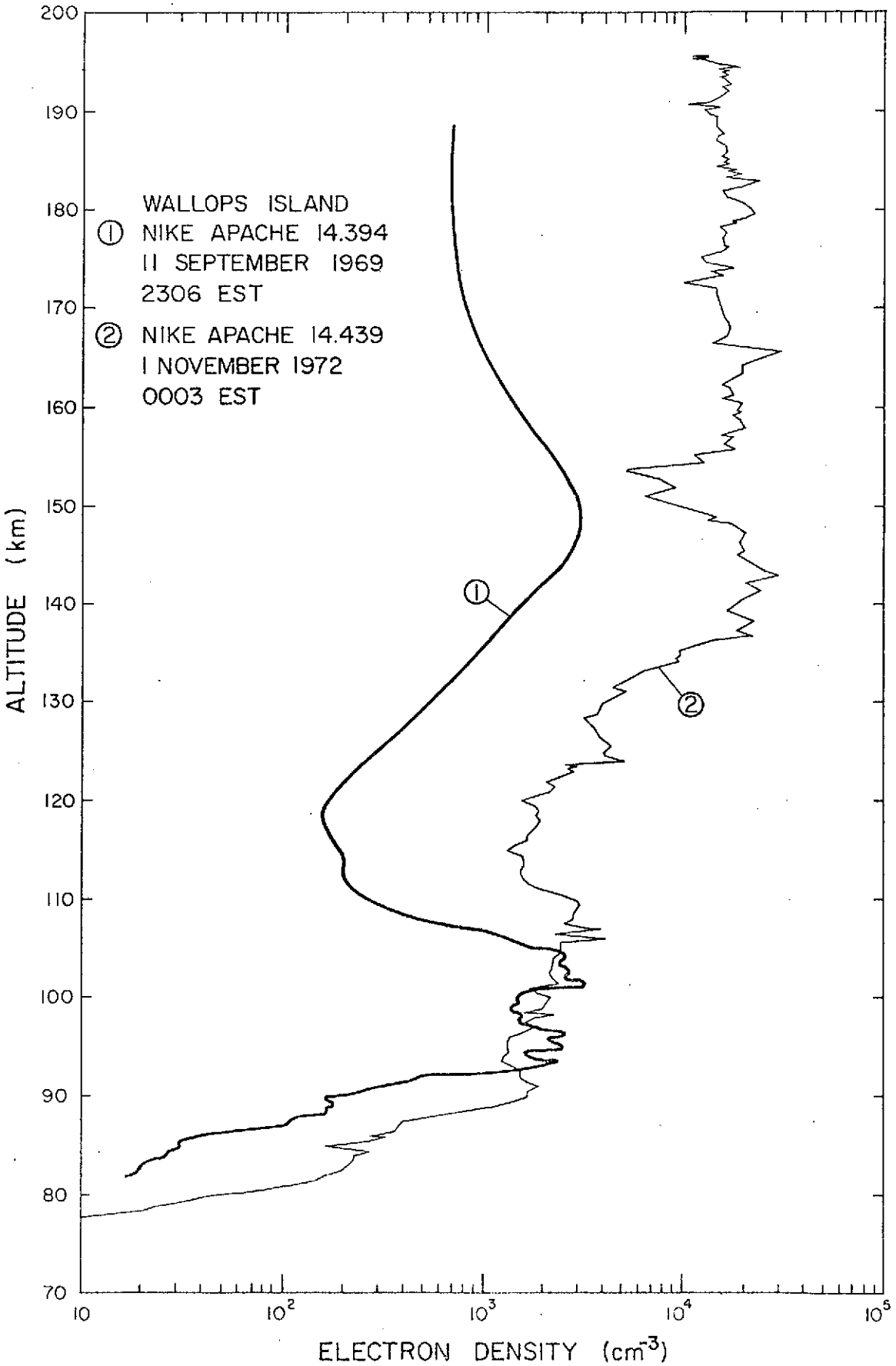
WALLOPS ISLAND
① NIKE APACHE 14.394
11 SEPTEMBER 1969
2306 EST
② NIKE APACHE 14.439
1 NOVEMBER 1972
0003 EST
ALTITUDE (km)
ELECTRON DENSITY (cm⁻³)
200
190
180
170
160
150
140
130
120
110
100
90
80
70
10
10²
10³
10⁴
10⁵

Figure 2

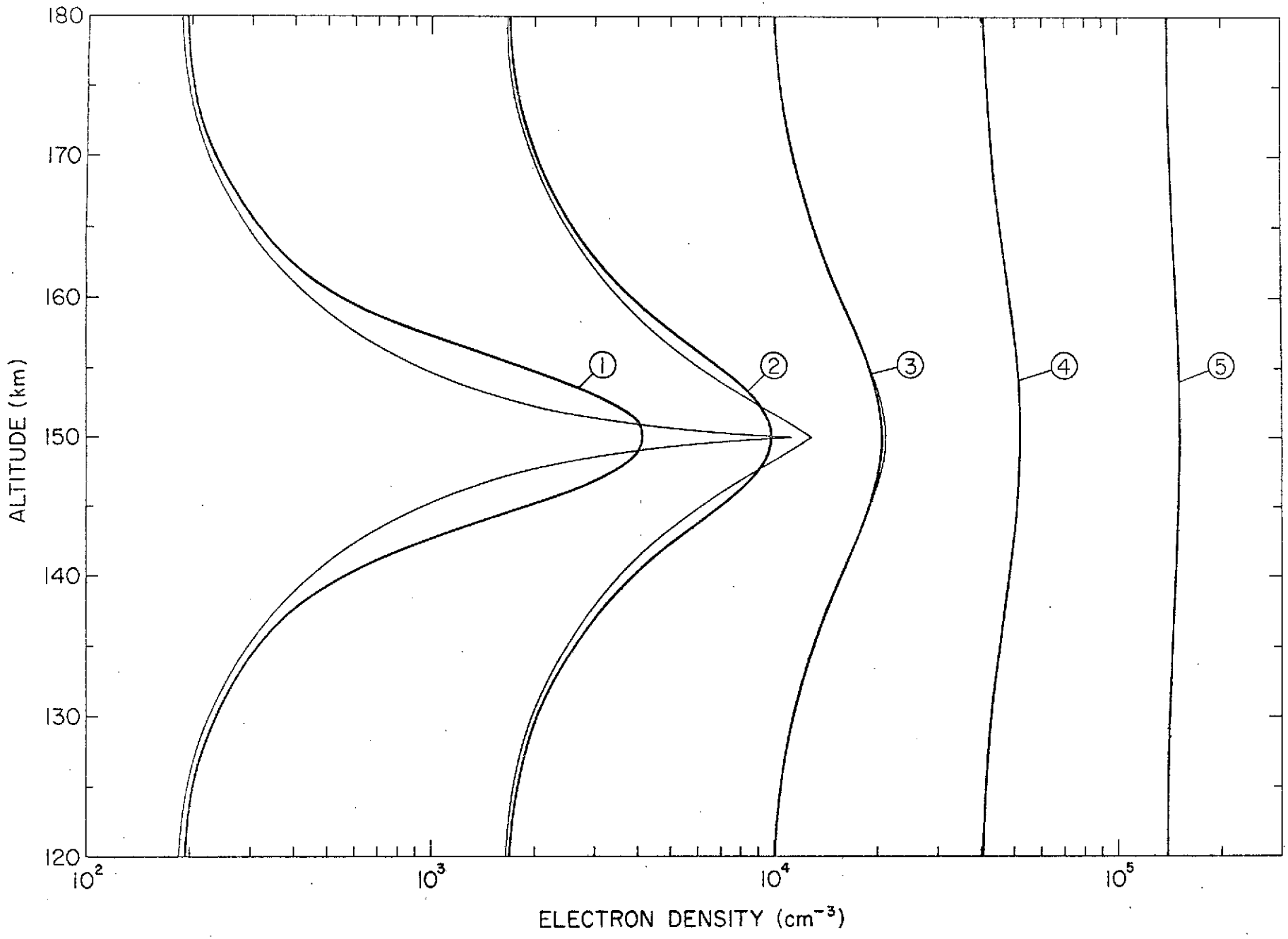
180
170
160
150
140
130
120
ALTITUDE (km)
10^2
10^3
10^4
10^5
ELECTRON DENSITY (cm^{-3})
1
2
3
4
5

Figure 3

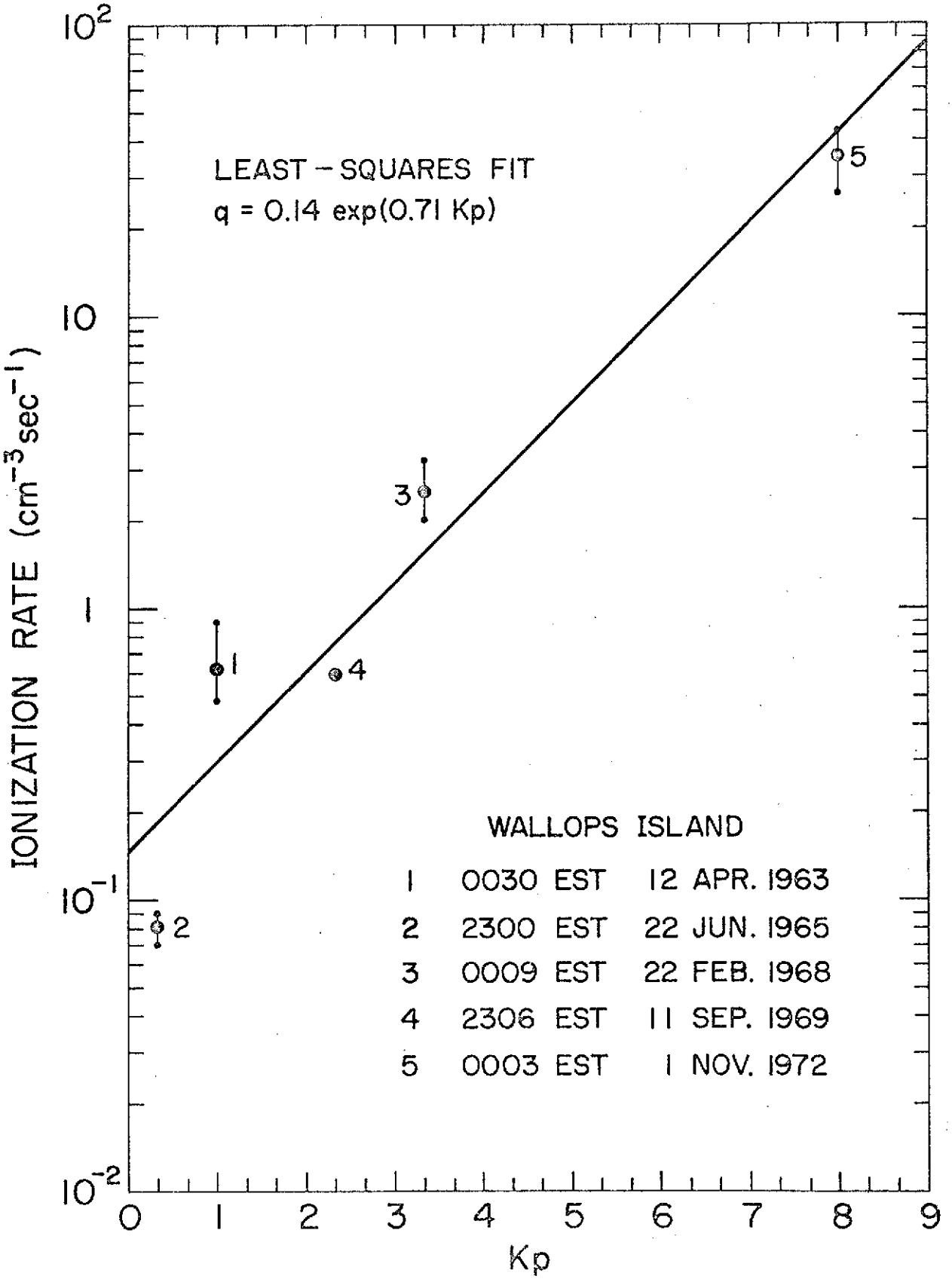
LEAST – SQUARES FIT
q = 0.14 exp(0.71 Kp)
WALLOPS ISLAND
1 0030 EST 12 APR. 1963
2 2300 EST 22 JUN. 1965
3 0009 EST 22 FEB. 1968
4 2306 EST 11 SEP. 1969
5 0003 EST 1 NOV. 1972
IONIZATION RATE (cm⁻³sec⁻¹)
Kp
10²
10
1
10⁻¹
10⁻²
0 1 2 3 4 5 6 7 8 9

Figure 4